

Thermo- and pH-Responsive Polymer Derived from Methacrylamide and Aspartic Acid

Chunhui Luo, Yu Liu, and Zhibo Li*

Beijing National Laboratory for Molecular Sciences (BNLMS), Institute of Chemistry, Chinese Academy of Sciences, Beijing 100190, China

Received July 8, 2010; Revised Manuscript Received August 28, 2010

ABSTRACT: A new type of thermo- and pH-responsive homopolymer was synthesized using reversible addition–fragmentation chain transfer (RAFT) polymerization. A novel functional methacrylamide monomer bearing α -aspartic acid derivative in the side chain, i.e., *N*-methacryloyl-*L*- β -isopropylasparagine benzyl ester (MA-iAsn-OBen), was first synthesized. Three poly(*N*-methacryloyl-*L*- β -isopropylasparagine benzyl ester)s [poly(MA-iAsn-OBen)] with controllable molecular weight and narrow molecular weight distribution were then prepared using RAFT polymerization. Selective removal of benzyl groups produced poly(*N*-methacryloyl-*L*- β -isopropylasparagine) [poly(MA-iAsn-OH)], which displayed a reversible lower critical solution temperature (LCST) in water. In addition, the LCST can be adjusted from 29 to 60 °C by changing solution pH values, salt concentrations, and polymer molecular weights. Using macromolecular chain transfer agent and RAFT polymerization, we prepared well-defined amphiphilic mPEG₄₅-*b*-poly(MA-iAsn-OBen)₅₃ diblock copolymer and double hydrophilic block copolymer [mPEG₄₅-*b*-poly(MA-iAsn-OH)₅₃]. The latter showed a thermo-induced self-assembly in water due to collapse of poly(MA-iAsn-OH) segment. We found that mPEG₄₅-*b*-poly(MA-iAsn-OH)₅₃ was soluble at room temperature while formed vesicles above the LCST of poly(MA-iAsn-OH)₅₃.

Introduction

Environmentally responsive polymers are termed “smart” materials, which can respond to external stimuli, such as temperature, pH, multivalent ions, ionic strength, and biomolecules, to induce substantial changes of material properties. These smart materials have found extensive applications in tissue engineering, drug delivery, bioseparations, biosensors, and nanomedicines.^{1–5} In particular, polymers that can respond to multiple external stimuli are of particular interest to constructing high-ordering and hierarchical supramolecular structures. Generally, different polymeric units that have distinct responsive moieties were incorporated into one copolymer system, which will display multiple responsive mechanisms. Among them, a widely studied dual-responsive system is thermo- and pH-responsive copolymers.^{6–12} The critical responsive pH and temperature can be adjusted through variation of copolymer constitutions, compositions, and architectures, etc. Such a dual responsive mechanism certainly can offer additional control over resulting supramolecular assembly structures as well as their functionalities.

Recently, much attention has been devoted to preparing polymers containing amino acids due to their biocompatibilities as well as their feasibility to create high-ordered structures.^{13–19} Although these hybrid copolymers can be prepared via various methods,^{20,21} great effort has been paid to the controlled/living radical polymerization (CRP).^{15,19,22–32} The primary reason is that CRP has high tolerance for various functional groups and precise control over polymer composition and architecture.^{33,34} For example, van Hest et al. synthesized a methacrylate-functionalized monomer bearing the short peptide sequence (VPGVG) in the side chain using ATRP and found that these polymers had dual pH- and thermo-sensitivity.^{15,23,24} The Endo group have studied the synthesis and properties of polymers containing different

amino acids in the side chains for many years.^{27–29,35–38} For example, they developed novel thermo-responsive (co)polymers containing a *N*-acryloyl-*L*-proline methyl ester (A-Pro-OMe) unit.^{27,35–37} They first reported RAFT polymerization of A-Pro-OMe and obtained well-defined thermo-responsive polymers, whose phase separation temperature can be tuned simply by copolymerization with hydrophilic monomers such as *N,N*-dimethylacrylamide (DMA)²⁷ and *N*-acryloyl-*L*-proline (A-Pro-OH).³⁶ Later, they investigated structures and chiroptical properties of thermo-responsive block copolymers containing *L*-proline moieties.³⁵ Most recently, Mori and co-workers reported dual-stimuli responsive block copolymers consisting of a thermo-responsive segment [poly(A-Pro-OMe)] and a weak anionic polyelectrolyte [poly(A-Pro-OH)].³⁶ In particular, they found that poly(A-Pro-OMe)-*b*-poly(*N*-acryloyl-4-*trans*-hydroxy-*L*-proline) displayed lower critical solution temperature (LCST) and upper critical solution temperature (UCST).³⁷ Also, McCormick and co-workers studied the self-assembly of multistimuli responsive block copolymers containing poly(*N*-acryloylalanine) and poly(*N*-acryloylvaline) using RAFT polymerization.^{25,26} The O'Reilly group studied the formation of micelle from amphiphilic block copolymers containing amino acids as side chains and self-assembly of amphiphilic chiral poly(amino acid) star polymers.^{17,18} Moreover, Adams and Young reported formation of vesicle from poly(ethylene oxide)-*b*-poly(methacryloyl side-chain peptides).¹⁴ However, to the best of our knowledge, only two groups of amino acids related poly(meth)acryl derivatives exhibit thermo-responsive properties. One is elastin-based (co)polymers, and the other is proline-based (co)polymers. Therefore, we are interested in developing new types of functional polymers containing α -amino acids as side chains and hope to expand the natural α -amino acids as functional groups to construct dual-stimuli responsive polymeric materials.

Herein, we attempted to incorporate thermo-responsive and pH-sensitive unit into a single molecule and utilized CRP to

*Corresponding author. E-mail: zbli@iccas.ac.cn.

prepare well-defined (co)polymers. We first designed a new vinyl monomer, namely *N*-methacryloyl-*L*- β -isopropylasparagine benzyl ester (MA-*i*Asn-OBen). The side chain of this monomer was *L*-aspartic acid derivative, in which the β -carboxyl group was converted into isopropyl amide group to mimic the structure of *N*-isopropylacrylamide for the purpose of thermo-responsive property. To reach a good control over the balance between hydrophobicity and hydrophilicity, we kept the $-\text{COOH}$ group in order to have pH sensitivity. Then we employed RAFT polymerization followed by selective removal of benzyl ester groups to obtain target polymers. We also investigated the aqueous solution properties of poly(MA-*i*Asn-OH) homopolymers and double hydrophilic mPEG₄₅-*b*-poly(MA-*i*Asn-OH)₅₃ diblock copolymer.

Experimental Section

Materials. Boc-*L*-Asp-OBen, dicyclohexylcarbodiimide (DCC), and 4-(dimethylamino)pyridine (DMAP) were purchased from GL Biochem (Shanghai) Ltd. and used as received. Isopropylamine (99%) and monomethoxypoly(ethylene glycol) (mPEG₄₅, $M_n = 2000$ g/mol) were obtained from Aldrich. All organic solvents were purchased from Beijing Chemical Co. Other reagents were purchased from Aladdin and used as received unless otherwise stated. 2,2'-Azobis(isobutyronitrile) (AIBN) was purified by recrystallization from methanol. Dichloromethane (DCM), tetrahydrofuran (THF), and *n*-hexane were dried by purging with nitrogen and passing through alumina columns prior to use. Deionized water was obtained from a Millipore Milli-Q purification unit. 2-Cyanoprop-2-yl(4-fluoro)dithiobenzoate (CPFDB),³⁹ 4-cyanopentanoic acid dithiobenzoate (CPADB),^{40,41} and mPEG₄₅-macro-CTA⁴² were synthesized according to reported procedures.

Synthesis of *N*-Methacryloyl- β -isopropylasparagine Benzyl Ester (MA-*i*Asn-OBen). *a. Synthesis of Boc-*L*- β -isopropylasparagine-OBen.* Boc-*L*-Asp-OBen (30 mmol, 10 g), DMAP (3 mmol, 0.36 g), and DCC (30 mmol, 6.18 g) were dissolved in 100 mL of anhydrous THF with magnetic stirring bar. While stirring vigorously, isopropylamine (30 mmol, 1.77 g) was added dropwise and then stirred for 24 h at RT. Dicyclohexylurea (DCU) was filtered off. Organic solvent was removed by rotary evaporation to give white crude product, which was purified by recrystallization using acetone/petroleum ether. Boc-*L*- β -isopropylasparagine-OBen was obtained in 80% yield. ¹H NMR (400 MHz, CDCl₃, TMS): $\delta = 7.35$ (C₆H₅, 5H, s), 6.25 (NHCH(CH₃)₂, 1H, s), 5.65 (NHCHCH₂, 1H, s), 5.21 (COOCH₂Ph, 2H, q), 4.84 (NHCHCH₂, 1H, m), 4.01 (NHCH(CH₃)₂, 1H, m), 2.62–3.06 (CHCH₂CO, 2H, m), 1.46 (OC(O)(CH₃)₃, 9H, s), 1.12 (NHCH(CH₃)₂, 6H, m).

*b. Synthesis of *L*- β -Isopropylasparagine-OBen.* Boc-*L*- β -isopropylasparagine-OBen (24 mmol, 8.16 g) was dissolved in 36 mL of anhydrous DCM at 0 °C followed with addition of TFA (0.1 mol, 9 mL). The mixture was slowly warmed up to RT and stirred for 2 h. An additional 100 mL of DCM was then added. The solution was washed with saturated NaHCO₃ and NaCl solution twice each. The organic layer was dried over anhydrous MgSO₄, and the solvent was then removed by rotary evaporation. The isolated yield was 95%. ¹H NMR (400 MHz, CDCl₃, TMS): $\delta = 7.78$ (NH₂CHCH₂, 2H, d), 7.35 (C₆H₅, 5H, s), 6.25 (NHCH(CH₃)₂, 1H, s), 5.21 (COOCH₂Ph, 2H, q), 4.01 (NHCH(CH₃)₂, 1H, m), 3.85 (NH₂CHCH₂, 1H, m), 2.62–3.06 (CHCH₂CO, 2H, m), 1.12 (NHCH(CH₃)₂, 6H, m).

*c. Synthesis of *N*-Methacryloyl-*L*- β -isopropylasparagine Benzyl Ester (MA-*i*Asn-OBen).* *L*- β -Isopropylasparagine-OBen (24 mmol, 6.33 g) and triethylamine (30 mmol, 3.03 g) were dissolved in 60 mL of anhydrous DCM, and the solution was cooled to 0 °C using an ice bath. Methacryloyl chloride (24 mmol, 2.51 g) dissolved in 10 mL of anhydrous DCM was added dropwise over 15 min. The mixture was slowly warmed up to RT and stirred for 24 h. The precipitated ammonium salt was removed by filtration. The DCM solution was subsequently washed with 1 M HCl and saturated NaHCO₃ solution twice each followed with saturated NaCl

solution once. The organic layer was dried over anhydrous MgSO₄, and the solvent was removed via rotary evaporator to give crude product. The crude product was subsequently purified by recrystallization three times using THF/petroleum ether. The isolated yield was 44%. ¹H NMR (400 MHz, CDCl₃, TMS): $\delta = 7.35$ (C₆H₅, 5H, s), 7.22 (NHCHCH₂, 1H, s), 6.41 (NHCH(CH₃)₂, 1H, s), 5.78 and 5.38 (CH₃CH=CCH₃, 1H, s and 1H, s), 5.21 (COOCH₂Ph, 2H, q), 4.84 (NHCHCH₂, 1H, m), 4.01 (NHCH(CH₃)₂, 1H, m), 2.62–3.06 (CHCH₂CO, 2H, m), 1.97 (CH₂=CCH₃, 3H, s), 1.12 (NHCH(CH₃)₂, 6H, m). ¹³C NMR (400 MHz, CDCl₃): $\delta = 172.01$ (COOCH₂), 169.31 (CONHCHCH₂), 168.14 (CONHCH(CH₃)₂), 139.10 (CH₂=CCH₃), 135.46 (ArC-1), 128.68 (ArC-2, ArC-3, and ArC-4), 120.92 (CH₂=CCH₃), 66.97 (CH₂Ar), 49.51 (NHCHCH₂), 41.76 (NHCH(CH₃)₂), 36.07 (CHCH₂CONH), 22.57 (CH(CH₃)₂), 18.47 (CH₂=CCH₃). High-resolution mass spectrum (HRMS): m/z calcd for C₁₈H₂₄N₂O₄ [M + H]⁺ 333.1814; found 333.1809. Anal. Calcd for C₁₈H₂₄N₂O₄: C, 65.04; H, 7.28; N, 8.43. Found: C, 65.07; H, 7.25; N, 8.32.

Synthesis of Poly(MA-*i*Asn-OBen) Homopolymers. All polymerizations of MA-*i*Asn-OBen were performed in a degassed sealed tube using CPFDB as the chain transfer agent (CTA) and AIBN as the initiator. The initial monomer-to-CTA ratio ([M]₀/[CTA]₀) was varied between 50 and 500 while the initial CTA-to-initiator ratio ([CTA]₀/[I]₀) was held constant at 2:1. A representative example for RAFT polymerization of MA-*i*Asn-OBen monomer was as follows: MA-*i*Asn-OBen (332 mg, 1 mmol), CPFDB (2.39 mg, 0.01 mmol), AIBN (0.82 mg, 0.005 mmol), and methanol (1 mL) were charged into a dry ampule. The solution was then deoxygenated using three freeze–evacuate–thaw cycles before the ampule was flame-sealed under vacuum. The ampule was then immersed into oil bath at 60 °C for 24 h. The polymerization was stopped by rapid cooling and exposure solution to air followed with methanol dilution. The solution was sampled for ¹H NMR and GPC measurements. The remaining product was precipitated using excess ethyl ether, and the precipitate was collected and dried in a vacuum. Conversion was assessed using ¹H NMR based on eq 1, where *I*_{5.78} and *I*_{5.38} are the integral of vinyl protons of CH₂=CCH₃ in MA-*i*Asn-OBen monomer, and *I*_{5.21} is the integral of methylene protons resonance of COOCH₂Ph in poly(MA-*i*Asn-OBen) polymer and MA-*i*Asn-OBen monomer. The conversion was 63%, determined from ¹H NMR.

$$\text{conversion} = (I_{5.21} - I_{5.78} - I_{5.38})/I_{5.21} \quad (1)$$

Synthesis of Block Copolymer. mPEG₄₅-CTA was used as chain transfer agent for preparing diblock copolymer of mPEG₄₅-*b*-poly(MA-*i*Asn-OBen). The polymerization was carried out in methanol with an initial monomer concentration of 1.0 M at 60 °C with AIBN as the initiator. The [macroCTA]₀:[AIBN]₀ ratio was maintained at 2, and [M]₀:[mPEG₄₅-CTA] ratio was 50. The procedure of making block copolymer was similar to homopolymer described above except that mPEG₄₅-CTA was used. The obtained M_n from GPC/LS was 17.2 kDa with PDI = 1.11. The DP of poly(MA-*i*Asn-OBen) was 53 determined from ¹H NMR using known mPEG₄₅ as reference.

Removal of Benzyl Ester. The conversion of poly(MA-*i*Asn-OBen) to poly(MA-*i*Asn-OH) was carried out by the standard method following literature procedure.^{43–45} 100 mg of poly(MA-*i*Asn-OBen) and a trace of ascorbic acid were dissolved in 1 mL of TFA at 0 °C, and then 0.5 mL of HBr/acetic acid (33%) solution was added. After stirring at RT for 2 h, 20 mL of diethyl ether was added. The precipitated polymer was dissolved in water and then dialyzed again in water for 72 h. After being lyophilized, the target homopolymer, poly(MA-*i*Asn-OH), was obtained in 85% yield. A similar deprotection procedure was applied for copolymers. Success of deprotection was confirmed from ¹H NMR characterization and GPC measurement. The GPC/LS measurement of mPEG₄₅-*b*-poly(MA-*i*Asn-OH)₅₃ was carried out after silylation of the free carboxylic groups with trimethylchlorosilane⁴⁶ ($M_n = 15.1$ kDa with PDI = 1.14).

Preparation of Copolymer Solutions. mPEG₄₅-*b*-poly(MA-*i*Asn-OH)₅₃ diblock was dissolved directly in DI water ($c = 1$ mg/mL). The solution pH was adjusted to desired values using 0.1 M HCl or NaOH for LCST, DLS, and cryo-TEM measurements.

Characterization. ¹H NMR and ¹³C NMR spectra were recorded on a Bruker AV400 FT-NMR spectrometer. High-resolution mass spectrometry (HRMS) was recorded on a Bruker Daltonics Inc. APEX II FT-ICRMS spectrometer. Elemental analysis was carried out using a Flash EA 1112 analyzer. CD spectra were recorded on an Applied Photophysics Chirascan CD spectrometer. Tandem gel permeation chromatography/light scattering (GPC/LS) was done at 50 °C using an SSI pump connected to Wyatt Optilab DSP and Wyatt DAWN EOS light scattering detectors with 0.02 M LiBr in DMF as eluent at flow rate of 1.0 mL/min. Dynamic light scattering (DLS) measurements were performed using LLS spectrometer (ALV/DLS/SLS-5322F) equipped with a multi- τ digital time correlator (ALV5000) and a He-Ne Laser ($\lambda = 632.8$ nm) at an angle of 90°. All solutions were filtered through a 0.45 μ m PVDF filter prior to measurements. The LCSTs were measured by monitoring the transmittance of a 500 nm light beam through a quartz sample cell at concentration of 1 mg/mL on a TU-1901 (Beijing Purkinje General Instrument Co. Ltd.) UV-vis spectrophotometer equipped with a temperature controller system (Peltier Temperature Controller-2). The solution was heated or cooled at rate of 1 °C/min between 20 and 70 °C. LCST was determined at 50% transmittance.⁹ For cryogenic transmission electron microscopy (cryo-TEM) characterization, samples were prepared in a controlled environment vitrification system (CEVS) at preset temperature. Block copolymer solution was annealed in the CEVS system for 10 min at each temperature prior to sample preparation. Typically, a 5 μ L sample solution was loaded onto a carbon-supported lacey TEM grid, which was held by tweezers. The excess solution was blotted with a piece of filter paper, resulting in the formation of thin films suspended the mesh holes, and the samples were quickly plunged into a reservoir of liquid ethane (cooled by liquid nitrogen) at its melting temperature. The vitrified samples were then stored in liquid nitrogen until they were transferred to a cryogenic sample holder (Gatan 626) and examined using a JEM 2200FS TEM (200 keV) at about -174 °C. The phase contrast was enhanced by underfocus. The images were recorded on a Gatan multiscan CCD and processed with Digital Micrograph.

Results and Discussion

Synthesis of MA-*i*Asn-OBen Monomer. The synthesis of polymerizable MA-*i*Asn-OBen monomer is outlined in Scheme 1. An orthogonal protected L-aspartic acid (Boc-L-Asp-OBen) as precursor was first coupled with isopropylamine to give Boc-L- β -isopropylasparagine-OBen. Selective removal of Boc-protective group using TFA produced L- β -isopropylasparagine-OBen, which subsequently reacted with methacryl chloride to produce target MA-*i*Asn-OBen monomer, whose structure was verified using ¹H NMR, ¹³C NMR (Figure 1), elemental analysis, and HRMS. ¹H NMR characterization showed that the integral ratio of proton resonance of $I_a:I_b:I_c:I_d:I_e:I_f:I_g:I_h:I_i:I_j$ is equal to 2:3:2:5:1:2:1:6:1:1 (Figure 1a), which agreed well with its corresponding structure. The ¹³C NMR spectrum shown in Figure 1b displayed the expected resonance and further confirmed successful synthesis of target monomer. HRMS and elemental analysis results were consistent well with theoretical values.

RAFT Polymerization of MA-*i*Asn-OBen. For understanding the relationship between physical properties and polymer structures, it is always desirable to make (co)polymers with controlled molecular weights and narrow molecular weight distribution (MWD). Considering the target MA-*i*Asn-OBen monomer containing amino acid unit and amide bond, we employed RAFT polymerization, which has been shown to have good control over such types of monomers.^{26,27} Previous research

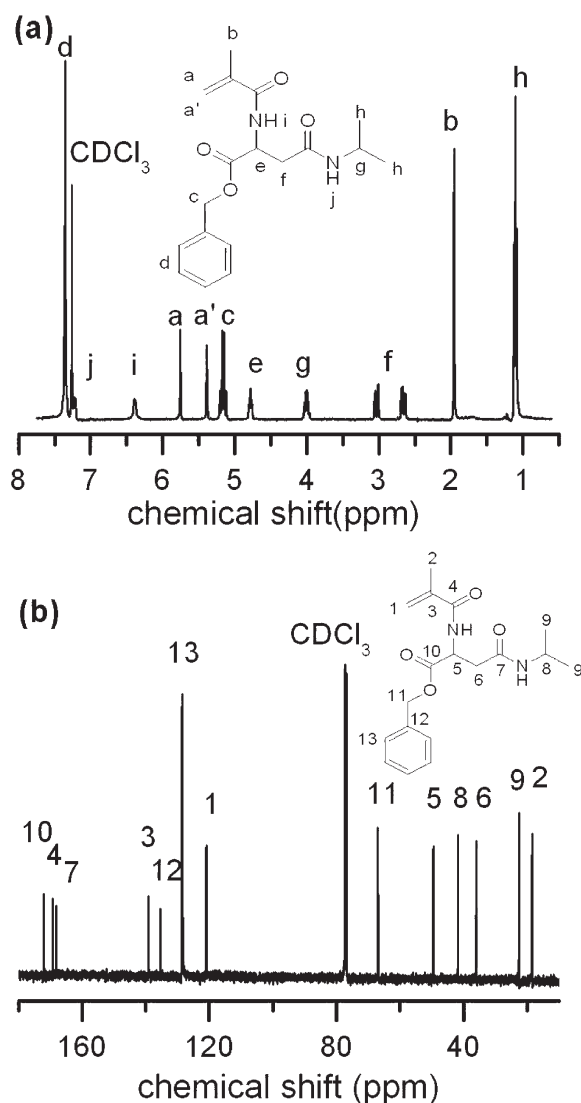
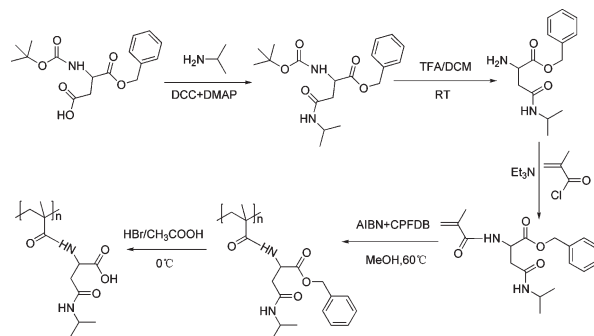


Figure 1. (a) ¹H NMR and (b) ¹³C NMR spectra of *N*-methacryloyl- β -isopropylasparagine benzyl ester (MA-*i*Asn-OBen) in CDCl₃.

Scheme 1. Synthetic Route to Poly(*N*-methacryloyl- β -isopropylasparagine) [Poly(MA-*i*Asn-OH)]



demonstrated that methanol and CPFDB were efficient for RAFT polymerization of methacrylate-functionalized monomers.^{39,47} Hence, we applied CPFDB as CTA to polymerize MA-*i*Asn-OBen monomer in methanol and prepared three poly(MA-*i*Asn-OBen) homopolymers with narrow MWD (Table S1). The obtained poly(MA-*i*Asn-OBen) homopolymers were found to be soluble in most organic solvents such as THF, DMSO, DMF, and methanol, etc., but insoluble in water.

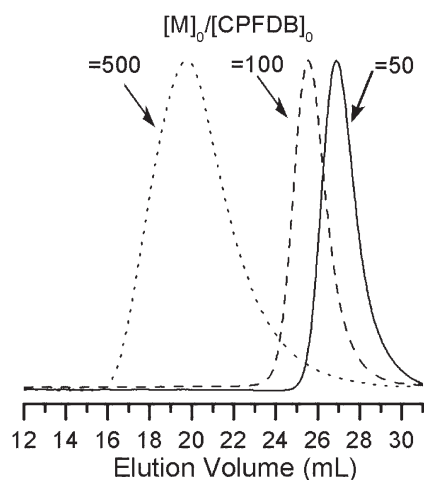


Figure 2. GPC traces of poly(MA-iAsn-OBen) at different $[M]_0/[CPFDB]_0$ ratios.

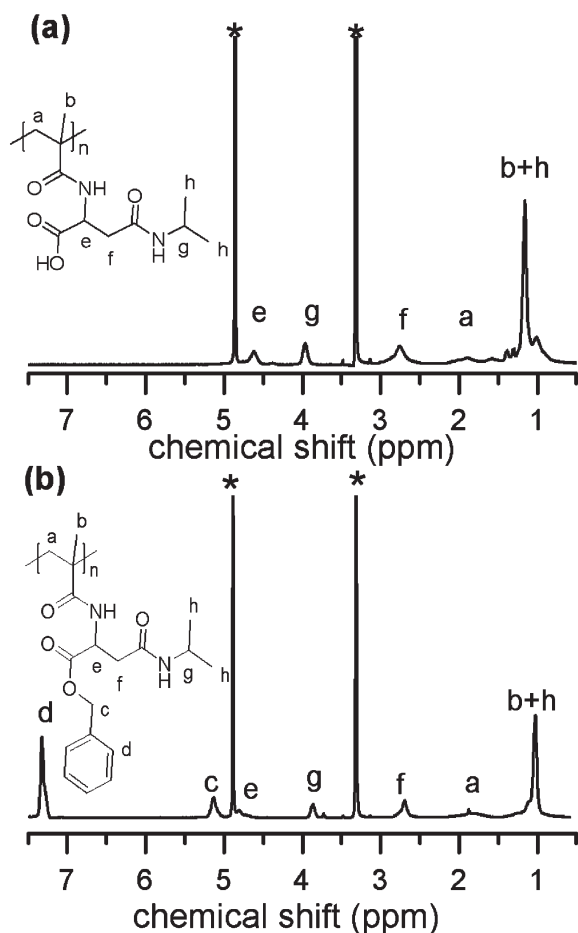


Figure 3. ^1H NMR spectra of (a) poly(*N*-methacryloyl- L - β -isopropyl-asparagine)₅₀ [poly(MA-iAsn-OH)₅₀] and (b) poly(*N*-methacryloyl- β -isopropylasparagine benzyl ester)₅₀ [poly(MA-iAsn-OBen)₅₀] in CD_3OD . The peaks marked with asterisks indicate solvents.

Figure 2 shows the GPC traces of the poly(MA-iAsn-OBen) prepared at different $[\text{monomer}]_0/[\text{CTA}]_0$ ratios with $[\text{CTA}]_0/[\text{AIBN}]_0 = 2$. For these three polymerizations, the conversions were around 60% (Table S1). The molecular weight of poly(MA-iAsn-OBen) increased monotonically with $[\text{monomer}]_0/[\text{CTA}]_0$ ratio (Figure S2), and the MWD remained

Table 1. LCST of 0.1 wt % Aqueous Solutions of Poly(MA-iAsn-OH) Homopolymers at Different pH Values

samples	LCST/ $^{\circ}\text{C}$			
	pH 1	pH 2	pH 3	pH 4
poly(MA-iAsn-OH) ₂₉₅	turbid	29	38	53
poly(MA-iAsn-OH) ₅₀	41	49		
poly(MA-iAsn-OH) ₃₀	60			

narrow ($M_w/M_n = 1.11\text{--}1.24$). Apparently, RAFT polymerization of MA-iAsn-OBen showed controlled polymerization characteristic, which allowed a good control over molecular weight of poly(MA-iAsn-OBen) for subsequent solution phase behavior studies.

Figure 3b shows the ^1H NMR of poly(MA-iAsn-OBen). The characteristic resonances of poly(MA-iAsn-OBen) are easily identified, and their integral ratio of $I_a:I_{(b+h)}:I_c:I_d:I_e:I_f:I_g$ is close to 2:9:2:5:1:2:1 (Figure 3b), in good agreement with its corresponding chemical structure. Selective removal of benzyl ester from poly(MA-iAsn-OBen) produced target poly(MA-iAsn-OH) (Scheme 1), as the ^1H NMR spectrum shown in Figure 3a clearly verified the successful deprotection of the benzyl group. Compared to the ^1H NMR spectrum of poly(MA-iAsn-OBen) (Figure 3b), resonances of aromatic ($\delta = 7.3$ ppm) and methylene ($\delta = 5.2$ ppm) protons from benzyl group disappeared while other characteristic resonances as well as the integral ratio remained intact after deprotection. Furthermore, the ^1H NMR spectrum did not display unknown resonances, suggesting that removal of benzyl group did not introduce unexpected structures. The target poly(MA-iAsn-OH) homopolymers were found soluble in water at neutral pH and displayed a reversible LCST behaviors in water at low pH, as discussed below.

We employed circular dichroism (CD) spectroscopy to assess the optical activity of the polymer before and after deprotection in methanol at RT (Figure S1). Poly(MA-iAsn-OBen)₅₀ exhibits a negative CD signal at 206 nm and a positive CD signal at 234 nm with intensities of about $-32\,800$ and 2400 $\text{deg cm}^2 \text{dmol}^{-1}$, respectively. This result was similar to poly(A-Pro-OMe) systems reported by Endo and co-workers.^{35,36} After deprotection, the poly(MA-iAsn-OH)₅₀ exhibits a negative CD signal at 197 nm and a positive CD signal at 224 nm, and the intensities were changed to about $31\,000$ and 6000 $\text{deg cm}^2 \text{dmol}^{-1}$, respectively. These results were consistent with similar systems containing $-\text{COOH}$ in their side chain.^{48,49} Typically, the peak around 200 nm was attributed to the $\pi_2 \rightarrow \pi^*$ transition or the $n \rightarrow \sigma$ transition of the amide group, while the signals around 207 and 230 nm were attributed to the $n \rightarrow \pi^*$ transition of the carboxyl chromophore and $\pi_1 \rightarrow \pi^*$ transition of the amide chromophore, respectively.⁴⁹

Phase Separation of Poly(MA-iAsn-OH) in Aqueous Solution. After successfully preparing poly(MA-iAsn-OH), we started to investigate their physical properties in water. Three poly(MA-iAsn-OH) homopolymers with DP being 30, 50, and 295 were used for this study (Table 1). The samples were designated as poly(MA-iAsn-OH)_{*n*} with *n* representing the degree of polymerization (DP).

Initial experiments showed that these poly(MA-iAsn-OH) homopolymers were soluble at neutral pH without measurable LCST behaviors between room temperature and 100 $^{\circ}\text{C}$. The reason we assumed was due to the ionization of $-\text{COOH}$ groups, which are weak acid with $\text{p}K_a$ around 4.2.²⁶ At pH = 7, almost all $-\text{COOH}$ groups will dissociate into $-\text{COO}^-$ groups. Considering the contribution of ionic groups toward poly(MA-iAsn-OH) solubility, we decided to decrease the pH values in order to protonate $-\text{COO}^-$ group. We aim to

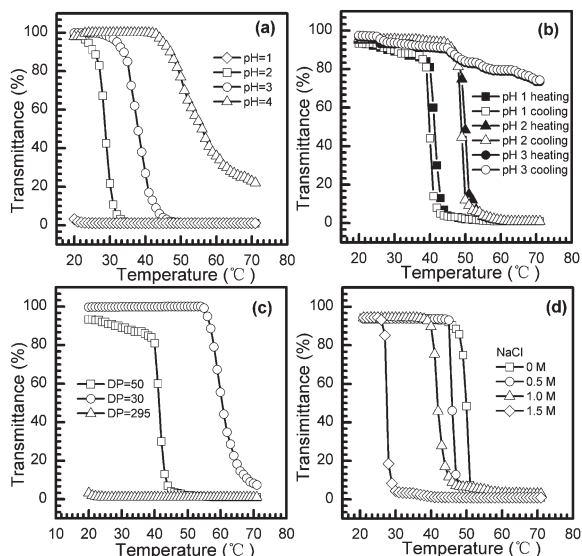


Figure 4. Temperature dependence of the transmittance at 500 nm of 1 mg/mL poly(MA-iAsn-OH) aqueous solutions: (a) poly(MA-iAsn-OH)₂₉₅ at different pH, (b) poly(MA-iAsn-OH)₅₀ at different pH, (c) poly(MA-iAsn-OH) at different DP at pH = 1, and (d) poly(MA-iAsn-OH)₅₀ solution at different NaCl concentrations with pH = 2.

find hydrophilic and hydrophobic balance among polymer backbone, isopropylamide, and $-\text{COOH}$ groups and ultimately realized a soluble–insoluble transition upon increase of temperature. Interestingly, poly(MA-iAsn-OH) homopolymers started to display a reversible soluble–insoluble phase transition with increase of temperature when $\text{pH} < 5$ (Figure 4). We also found that the LCST of poly(MA-iAsn-OH) varies with molecular weight and solution ionic strength. We thus systematically explored the roles of polymer molecular weight, pH value, and ion strength on polymers LCST behaviors in water as discussed below.^{23,36,50}

Figure 4a shows the solution turbidity of poly(MA-iAsn-OH)₂₉₅ aqueous solution (1 mg/mL) versus temperature at different pH. When pH = 1, the LCST of poly(MA-iAsn-OH)₂₉₅ was not obtainable as we did not have cooling unit in the turbidity apparatus. Its LCST seemed below room temperature (~ 25 °C). When pH = 2, poly(MA-iAsn-OH)₂₉₅ showed a soluble–insoluble transition at 29 °C. The phase transition started at 25 °C with 90% transmittance and ended at 32 °C with 5% transmittance, which gave a phase transition range about 7 deg. When the pH was increased to 3 and 4, poly(MA-iAsn-OH)₂₉₅ had its LCST increased to 38 and 53 °C, respectively (Figure 4a). Further increasing solution pH to 5, poly(MA-iAsn-OH)₂₉₅ did not show distinguishable LCST. In contrast, poly(MA-iAsn-OH)₅₀ at pH = 1 had LCST of 41 °C (Figure 4b), which was much higher than that of poly(MA-iAsn-OH)₂₉₅ under the same conditions. When pH = 2, poly(MA-iAsn-OH)₅₀ underwent a phase transition around 49 °C, in contrast to 29 °C for poly(MA-iAsn-OH)₂₉₅. At pH = 3, poly(MA-iAsn-OH)₅₀ did not display a sharp LCST transition, and its solution still had 70% transmittance even at 70 °C (Figure 4b). Apparently, the LCST of poly(MA-iAsn-OH) strongly depended on solution pH. We attributed this to the presence of ionizable $-\text{COOH}$ groups, which endowed ionic nature to poly(MA-iAsn-OH). As a result, the LCST of poly(MA-iAsn-OH) is primarily determined by the balance between thermo-dependent hydrophobic unit and ionizable $-\text{COOH}$ groups. The higher the solution pH, the more ionic $-\text{COO}^-$ groups, which improve the polymer solubility.^{23,26,36} As a result, increase of phase transition temperature was required to

compensate the enhanced hydrophilicity from ionic $-\text{COO}^-$ groups along increase of solution pH. Figure 4b also shows the cooling histogram of transmittance vs temperature, suggesting reversible soluble–insoluble phase transition for poly(MA-iAsn-OH) system. The LCST determined from cooling was about 1 deg lower than that determined from the heating ramp. The hysteresis between heating and cooling cycles most likely arose from the inter- and intrachain hydrogen bonding at insoluble status as suggested in literature reports.^{51,52}

Our experiments showed that the LCST of poly(MA-iAsn-OH) decreased with increasing polymer molecular weight (Figure 4c), which is consistent with literature reports.^{23,47,53} For the example of pH = 1, poly(MA-iAsn-OH)₂₉₅ has LCST below room temperature, while poly(MA-iAsn-OH)₃₀ and poly(MA-iAsn-OH)₅₀ has LCST around 60 and 41 °C, respectively. This trend was similar to that of PNIPAM system (from 32 to 70 °C).⁵⁴ Generally, the molecular weight dependence of LCST could arise from several factors including polymer–solvent interaction, intramolecular interactions, and end-group contributions.⁵⁵ In particular, the end-group effect was significant for the low molecular weight samples and became less remarkable with increase of polymer chain length.^{54,55} Apparently, the end group from CTA would have significant influence on the LCST of poly(MA-iAsn-OH), as expected. However, we could not quantify the contribution of end group toward LCST given the available data. Meanwhile, we also note that the LCST variation range was just a few degrees for PNIPAM having same end group but different molecular weight. Here, the LCST for poly(MA-iAsn-OH) spanned from at least 25 to 60 °C when DP changed from 295 to 30. Therefore, another possible contribution we assume might be the enhanced intramolecular hydrogen bonding between polar $-\text{NHCO}-$ and $-\text{COOH}$ groups when the poly(MA-iAsn-OH) chain length increases.

We also found that solution ionic strength can also affect the LCST of poly(MA-iAsn-OH) aqueous solutions (Figure 4d). Here, we chose NaCl as the additive salt for our studies. For 1 mg/mL aqueous solution of poly(MA-iAsn-OH)₅₀, addition of different amounts of NaCl progressively lowered its LCST from 49 without NaCl to 46, 42, and 28 °C at $[\text{NaCl}] = 0.5, 1.0, \text{ and } 1.5 \text{ M}$, respectively. The underlying reason we believed was due to ionic nature of $-\text{COOH}$ groups. Since poly(MA-iAsn-OH) is a weak polyelectrolyte, the ionic strength can affect the degree of ionization, and consequently polymer solubility provided other parameters were identical. Therefore, addition of NaCl will decrease poly(MA-iAsn-OH) solubility in water, and corresponding LCST will decrease accordingly (Figure 4d).^{23,36}

It needs pointing out that the dual-responsive mechanism of poly(MA-iAsn-OH) arose from a single monomer bearing two distinct functional groups, so copolymerization was not necessary to obtain dual-stimuli-responsive property. An additional benefit was that we can rather easily prepare multiple-responsive polymer via copolymerization with other specific monomers.

Synthesis of mPEG₄₅-b-poly(MA-iAsn-OH)₅₃ Copolymer. We have demonstrated that poly(MA-iAsn-OH) homopolymer has dual thermo- and pH-responsive properties in water. We thought about using its stimuli mechanism to make responsive block copolymers, from which we can construct intelligent drug delivery systems. We chose mPEG₄₅-CTA to perform RAFT polymerization of MA-iAsn-OBen and obtained mPEG₄₅-b-poly(MA-iAsn-OBen). The $[\text{monomer}]_0/[\text{mPEG}_{45}\text{-CTA}]_0$ is 50, and conversion of monomer was $>95\%$ determined by ¹H NMR right after polymerization.

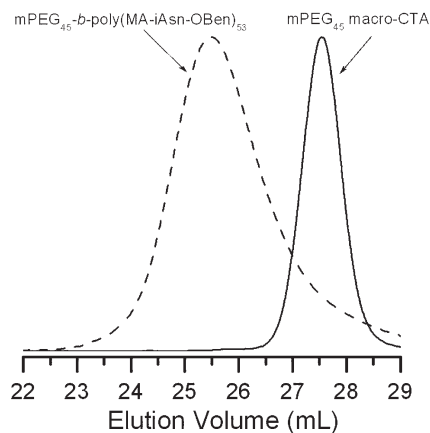


Figure 5. GPC traces of mPEG₄₅-CTA (solid) and mPEG₄₅-*b*-poly(MA-*i*Asn-OBen)₅₃ (dashed) diblock copolymer.

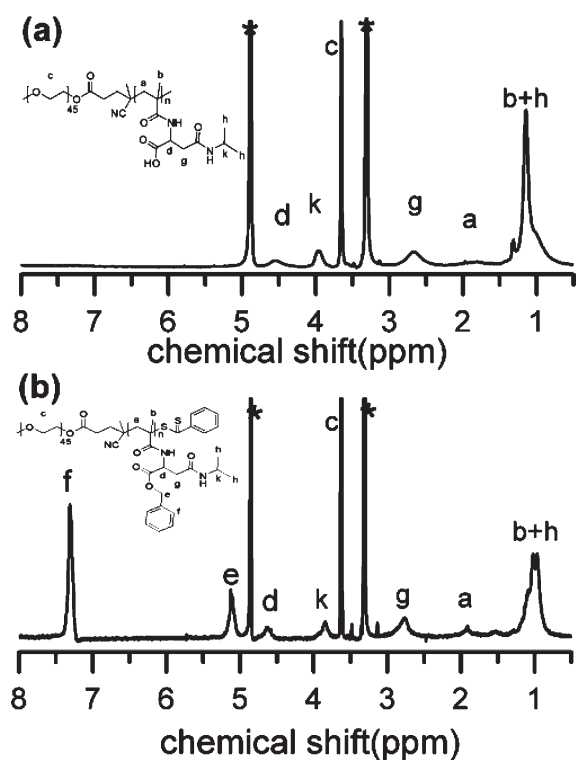


Figure 6. ¹H NMR spectra of (a) mPEG₄₅-*b*-poly(MA-*i*Asn-OH)₅₃ and (b) mPEG₄₅-*b*-poly(MA-*i*Asn-OBen)₅₃ diblock copolymer in CD₃OD. The peaks marked with asterisks indicate solvents.

Figure 5 compares the GPC traces of mPEG₄₅-CTA and mPEG₄₅-*b*-poly(MA-*i*Asn-OBen). Compared to mPEG₄₅-CTA, mPEG₄₅-*b*-poly(MA-*i*Asn-OBen) diblock had substantial decrease of elution volume, indicating a successful extension of polymer chain from mPEG₄₅-CTA. Although the GPC trace of mPEG₄₅-*b*-poly(MA-*i*Asn-OBen) diblock had a small shoulder peak at the low molecular region, we believed the shoulder was caused by inactive mPEG₄₅-CTA. Also, its contribution to diblock would be minimal as supported by the relative narrow molecular weight distribution of diblock (PDI = 1.11). From ¹H NMR (Figure 6b) of mPEG₄₅-*b*-poly(MA-*i*Asn-OBen) diblock, the DP of poly(MA-*i*Asn-OBen) block was calculated to be 53 given *M_n* of mPEG₄₅-CTA. The diblock will be designated as mPEG₄₅-*b*-poly(MA-*i*Asn-OBen)₅₃ for remaining text. On the basis of the monomer conversion and DP of poly(MA-*i*Asn-OBen),

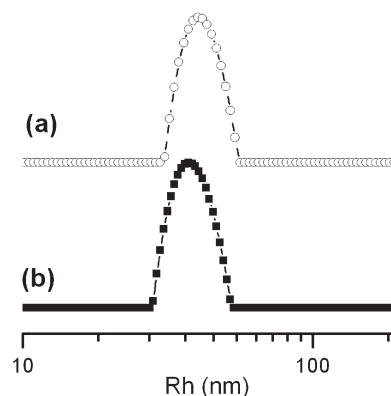


Figure 7. Apparent size distribution of aggregates formed from 0.1 wt % mPEG₄₅-*b*-poly(MA-*i*Asn-OH)₅₃ aqueous solution at (a) 60 °C with pH = 2 and (b) 50 °C with pH = 1. The scattering angle is 90°.

we can estimate that purity of mPEG₄₅-CTA was 95% (containing 5% inactive mPEG₄₅), which also explained the small shoulder observed in GPC trace (Figure 5). Moreover, the GPC/LS measurement gave *M_n* of diblock being 17.2 kDa, from which we can estimate the DP of poly(MA-*i*Asn-OBen) block was 46, which was smaller than NMR results.

The success of deprotection was confirmed from ¹H NMR as the resonances of benzyl group completely disappeared while other characteristic resonances as well as the integral ratio remained intact (Figure 6). We attempted to use hydrogenation to remove benzyl group, but could not obtain 100% deprotection. So we adopted a more aggressive HBr/acetic acid system to deprotect benzyl group.^{43,45} Although the ester linkage between mPEG₄₅ and poly(MA-*i*Asn-OBen)₅₃ is subject to acid catalyzed cleavage, we tried to control reaction conditions in order to minimize the possible side reaction. Our result showed that mPEG₄₅-*b*-poly(MA-*i*Asn-OH)₅₃ did not have substantial chain cleavage supported from ¹H NMR and GPC (Figure S3). Above all, the selective deprotection of benzyl group was successful to produce double hydrophilic mPEG₄₅-*b*-poly(MA-*i*Asn-OH)₅₃ diblock, which is soluble in water within all pH ranges at room temperature. Since poly(MA-*i*Asn-OH)₅₃ is thermo- and pH-responsive block, we expect it will form supramolecular aggregates at elevated temperature and low pH value. We then started to investigate the thermo-induced aqueous self-assembly of mPEG₄₅-*b*-poly(MA-*i*Asn-OH)₅₃.

Solution Behaviors of mPEG₄₅-*b*-poly(MA-*i*Asn-OH)₅₃ Diblock. Because of the thermo-responsive characteristic of poly(MA-*i*Asn-OH), mPEG₄₅-*b*-poly(MA-*i*Asn-OH)₅₃ will undergo a thermo-induced transition from double hydrophilic diblock to amphiphilic diblock upon temperature increase. We knew that poly(MA-*i*Asn-OH) displayed LCST behaviors only when most -COOH groups were protonated, so we mainly investigated the thermo-induced aqueous self-assembly of mPEG₄₅-*b*-poly(MA-*i*Asn-OH)₅₃ diblock at pH = 1 and 2. For 1 mg/mL aqueous solution of mPEG₄₅-*b*-poly(MA-*i*Asn-OH)₅₃ diblock, visual observation showed the solution became cloudy at elevated temperature when pH = 1 or 2.

We employed dynamic light scattering (DLS) to monitor scattering intensity and apparent aggregate size dependence on temperature (Figure S4a). The mPEG₄₅-*b*-poly(MA-*i*Asn-OH)₅₃ aqueous solution displayed LCST around 40 °C at pH = 1 and 48 °C at pH = 2, consistent well with corresponding homopolymer with DP = 50 (Figure 4). Also, the soluble-insoluble transition was reversible as indicated from DLS measurements (Figure S4a). In addition to scattering

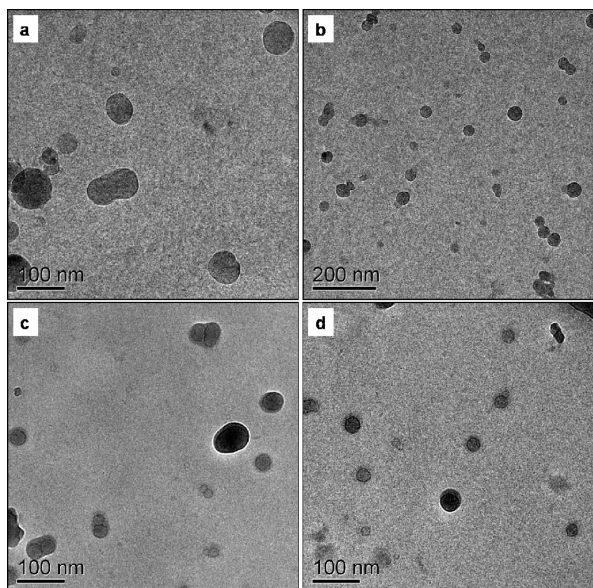


Figure 8. Cryo-TEM micrographs of assemblies formed from 0.1 wt % mPEG₄₅-*b*-poly(MA-iAsn-OH)₅₃ aqueous solution at (a, b) 50 °C with pH = 1 and (c, d) 60 °C with pH = 2.

intensity variation, the apparent aggregate sizes dependence on temperature was also determined from DLS (Figure S4b). When pH = 1, mPEG₄₅-*b*-poly(MA-iAsn-OH)₅₃ started to form large aggregates when $T > 35$ °C. The apparent hydrodynamic radius (R_h) was about 70 nm at 40 °C and decreased slightly to 37 nm at 50 °C. When pH = 2, mPEG₄₅-*b*-poly(MA-iAsn-OH)₅₃ started to form large aggregates when $T > 46$ °C. The apparent R_h of aggregates was about 240 nm at $T = 50$ °C and decreased slightly to 110 nm at 55 °C and down to 40 nm at 60 °C. Figure 7 shows the apparent size distribution of aggregates formed from mPEG₄₅-*b*-poly(MA-iAsn-OH)₅₃ (1 mg/mL) in aqueous solution at pH = 1 and 2. For pH = 1, mPEG₄₅-*b*-poly(MA-iAsn-OH)₅₃ diblock formed aggregates with R_h about 37 nm. At pH = 2, mPEG₄₅-*b*-poly(MA-iAsn-OH)₅₃ diblock formed larger aggregates at 50 °C, but similar aggregate sizes at 60 °C. The nanostructures of these aggregates at 50 °C (pH = 1) and 60 °C (pH = 2) were found to be vesicular assemblies from cryo-TEM (Figure 8). At pH = 1 and 50 °C, the vesicle diameters from cryo-TEM ranged from 40 to 100 nm (Figure 8a,b). At pH = 2 and 60 °C, the vesicles diameters were between 46 and 80 nm (Figure 8c,d).

Similar studies and characterization on amphiphilic mPEG₄₅-*b*-poly(MA-iAsn-OBen)₅₃ diblock showed that it also formed vesicles at same conditions (Figure S5). Note that we also observed some large aggregates around a few hundred nanometers for this diblock in addition to vesicles. The reason was probably because the thermo-sensitive poly(MA-iAsn-OH) block was the majority component. For this particular mPEG₄₅-*b*-poly(MA-iAsn-OH)₅₃ diblock, the weight fraction of poly(MA-iAsn-OH) was 84%. At such high hydrophobic content, formation of vesicle for mPEG₄₅-*b*-poly(MA-iAsn-OH)₅₃ was expected as supported from previous experiments and simulation studies, which showed that diblock with high weight fraction of hydrophobic block preferred forming vesicular structures in selective solvents.^{56,57}

Conclusion

In summary, we synthesized a new type of thermo- and pH-responsive poly(*N*-methacryloyl- β -isopropylasparagine) [poly(MA-iAsn-OH)] homopolymer based on methacrylamide and

aspartic acid via RAFT polymerization. We found that the LCST of poly(MA-iAsn-OH) in water increases with solution pH when pH < 5. Increase polymer chain length or solution salt concentration will decrease LCST for dilute poly(MA-iAsn-OH) aqueous solution. Using mPEG₄₅-CTA as macro-CTA, we made amphiphilic mPEG₄₅-*b*-poly(MA-iAsn-OBen)₅₃, which was converted into double hydrophilic mPEG₄₅-*b*-poly(MA-iAsn-OH)₅₃ diblock copolymer. The former formed vesicles in water, while the latter underwent a transition from polymer chain to vesicular assemblies upon increase of solution temperature. This new type of stimuli-responsive polymer prepared from a single monomer might be useful to prepare multiresponsive polymers for drug delivery and biomedical sensors applications.

Acknowledgment. This work was supported by the National Natural Science Foundation of China (20974112, 50821062). We thank Dr. Yi Shi for the help in RAFT agent synthesis and useful discussions.

Supporting Information Available: CD spectra, additional GPC, DLS, and cryo-TEM data, and NMR spectra. This material is available free of charge via the Internet at <http://pubs.acs.org>.

References and Notes

- Schmaljohann, D. *Adv. Drug Delivery Rev.* **2006**, *58*, 1655–1670.
- Kumar, A.; Srivastava, A.; Galaev, I. Y.; Mattiasson, B. *Prog. Polym. Sci.* **2007**, *32*, 1205–1237.
- Gil, E. S.; Hudson, S. M. *Prog. Polym. Sci.* **2004**, *29*, 1173–1222.
- Motornov, M.; Roiter, Y.; Tokarev, I.; Minko, S. *Prog. Polym. Sci.* **2010**, *35*, 174–211.
- Stuart, M. A. C.; Huck, W. T. S.; Genzer, J.; Muller, M.; Ober, C.; Stamm, M.; Sukhorukov, G. B.; Szleifer, I.; Tsukruk, V. V.; Urban, M.; Winnik, F.; Zauscher, S.; Luzinov, I.; Minko, S. *Nature Mater.* **2010**, *9*, 101–113.
- Zhang, L. Y.; Guo, R.; Yang, M.; Jiang, X. Q.; Liu, B. R. *Adv. Mater.* **2007**, *19*, 2988–2992.
- Andre, X.; Zhang, M. F.; Müller, A. H. E. *Macromol. Rapid Commun.* **2005**, *26*, 558–563.
- Twaites, B. R.; Alarcon, C. D.; Cunliffe, D.; Lavigne, M.; Pennadam, S.; Smith, J. R.; Gorecki, D. C.; Alexander, C. *J. Controlled Release* **2004**, *97*, 551–566.
- Fournier, D.; Hoogenboom, R.; Thijs, H. M. L.; Paulus, R. M.; Schubert, U. S. *Macromolecules* **2007**, *40*, 915–920.
- Klaikherd, A.; Nagamani, C.; Thayumanavan, S. *J. Am. Chem. Soc.* **2009**, *131*, 4830–4838.
- Ge, Z. S.; Xie, D.; Chen, D. Y.; Jiang, X. Z.; Zhang, Y. F.; Liu, H. W.; Liu, S. Y. *Macromolecules* **2007**, *40*, 3538–3546.
- Li, C.; Ge, Z.; Fang, J.; Liu, S. *Macromolecules* **2009**, *42*, 2916–2924.
- Geng, Y.; Discher, D. E.; Justynska, J.; Schlaad, H. *Angew. Chem., Int. Ed.* **2006**, *45*, 7578–7581.
- Adams, D. J.; Atkins, D.; Cooper, A. I.; Furzeland, S.; Trewin, A.; Young, I. *Biomacromolecules* **2008**, *9*, 2997–3003.
- Ayres, L.; Hans, P.; Adams, J.; Lowik, D.; van Hest, J. C. M. *J. Polym. Sci., Part A: Polym. Chem.* **2005**, *43*, 6355–6366.
- Vandermeulen, G. W. M.; Klok, H. A. *Macromol. Biosci.* **2004**, *4*, 383–398.
- Skey, J.; Hansell, C. F.; O'Reilly, R. K. *Macromolecules* **2010**, *43*, 1309–1318.
- Skey, J.; Willcock, H.; Lammens, M.; Du Prez, F.; O'Reilly, R. K. *Macromolecules* **2010**, *43*, 5949–5955.
- O'Reilly, R. K. *Polym. Int.* **2010**, *59*, 568–573.
- Kricheldorf, H. R. *Angew. Chem., Int. Ed.* **2006**, *45*, 5752–5784.
- Becker, M. L.; Liu, J. Q.; Wooley, K. L. *Chem. Commun.* **2003**, 180–181.
- Ayres, L.; Adams, P.; Lowik, D.; van Hest, J. C. M. *Biomacromolecules* **2005**, *6*, 825–831.
- Ayres, L.; Koch, K.; Adams, P.; van Hest, J. C. M. *Macromolecules* **2005**, *38*, 1699–1704.
- Ayres, L.; Vos, M. R. J.; Adams, P.; Shklyarevskiy, I. O.; van Hest, J. C. M. *Macromolecules* **2003**, *36*, 5967–5973.
- Lokitz, B. S.; Convertine, A. J.; Ezell, R. G.; Heidenreich, A.; Li, Y.; McCormick, C. L. *Macromolecules* **2006**, *39*, 8594–8602.

- (26) Lokitz, B. S.; York, A. W.; Stempka, J. E.; Treat, N. D.; Li, Y.; Jarrett, W. L.; McCormick, C. L. *Macromolecules* **2007**, *40*, 6473–6480.
- (27) Mori, H.; Iwaya, H.; Nagai, A.; Endo, T. *Chem. Commun.* **2005**, 4872–4874.
- (28) Mori, H.; Kato, I.; Matsuyama, M.; Endo, T. *Macromolecules* **2008**, *41*, 5604–5615.
- (29) Sanda, F.; Endo, T. *Macromol. Chem. Phys.* **1999**, *200*, 2651–2661.
- (30) Skey, J.; O'Reilly, R. K. *J. Polym. Sci., Part A: Polym. Chem.* **2008**, *46*, 3690–3702.
- (31) Evans, A. C.; Skey, J.; Wright, M.; Qu, W. J.; Ondeck, C.; Longbottom, D. A.; O'Reilly, R. K. *J. Polym. Sci., Part A: Polym. Chem.* **2009**, *47*, 6814–6826.
- (32) Zhao, F. B.; Liu, Z. L.; Feng, L.; Sun, J. P.; Hu, J. W. *Acta Polym. Sin.* **2009**, *2*, 166–172.
- (33) Matyjaszewski, K.; Xia, J. H. *Chem. Rev.* **2001**, *101*, 2921–2990.
- (34) Moad, G.; Rizzardo, E.; Thang, S. H. *Aust. J. Chem.* **2005**, *58*, 379–410.
- (35) Mori, H.; Iwaya, H.; Endo, T. *Macromol. Chem. Phys.* **2007**, *208*, 1908–1918.
- (36) Mori, H.; Kato, I.; Endo, T. *Macromolecules* **2009**, *42*, 4985–4992.
- (37) Mori, H.; Kato, I.; Saito, S.; Endo, T. *Macromolecules* **2010**, *43*, 1289–1298.
- (38) Sanda, F.; Abe, T.; Endo, T. *J. Polym. Sci., Part A: Polym. Chem.* **1997**, *35*, 2619–2629.
- (39) Benaglia, M.; Rizzardo, E.; Alberti, A.; Guerra, M. *Macromolecules* **2005**, *38*, 3129–3140.
- (40) Thang, S. H.; Chong, Y. K.; Mayadunne, R. T. A.; Moad, G.; Rizzardo, E. *Tetrahedron Lett.* **1999**, *40*, 2435–2438.
- (41) Mitsukami, Y.; Donovan, M. S.; Lowe, A. B.; McCormick, C. L. *Macromolecules* **2001**, *34*, 2248–2256.
- (42) Chong, Y. K.; Le, T. P. T.; Moad, G.; Rizzardo, E.; Thang, S. H. *Macromolecules* **1999**, *32*, 2071–2074.
- (43) Wang, H. B.; Chen, X. S.; Pan, C. Y. *Acta Polym. Sin.* **2008**, 161–167.
- (44) Ben-Ishai, D.; Berger, A. *J. Org. Chem.* **1952**, *17*, 1564–1570.
- (45) Motala-Timol, S.; Jhurry, D.; Zhou, J.; Bhaw-Luximon, A.; Mohun, G.; Ritter, H. *Macromolecules* **2008**, *41*, 5571–5576.
- (46) Gingter, S.; Bezdushna, E.; Ritter, H. *Macromolecules* **2010**, *43*, 3128–3131.
- (47) Deng, J.; Shi, Y.; Jiang, W.; Peng, Y.; Lu, L.; Cai, Y. *Macromolecules* **2008**, *41*, 3007–3014.
- (48) Lokitz, B. S.; Stempka, J. E.; York, A. W.; Li, Y. T.; Goel, H. K.; Bishop, G. R.; McCormick, C. L. *Aust. J. Chem.* **2006**, *59*, 749–754.
- (49) Morcellet-Sauvage, J.; Morcellet, M.; Loucheux, C. *Macromolecules* **1983**, *16*, 1564–1570.
- (50) Van Durme, K.; Rahier, H.; Van Mele, B. *Macromolecules* **2005**, *38*, 10155–10163.
- (51) Cheng, H.; Shen, L.; Wu, C. *Macromolecules* **2006**, *39*, 2325–2329.
- (52) Wu, C.; Wang, X. H. *Phys. Rev. Lett.* **1998**, *80*, 4092–4094.
- (53) Xia, Y.; Yin, X.; Burke, N. A. D.; Stöver, H. D. H. *Macromolecules* **2005**, *38*, 5937–5943.
- (54) Xia, Y.; Burke, N. A. D.; Stöver, H. D. H. *Macromolecules* **2006**, *39*, 2275–2283.
- (55) Furryk, S.; Zhang, Y. J.; Ortiz-Acosta, D.; Cremer, P. S.; Bergbreiter, D. E. *J. Polym. Sci., Part A: Polym. Chem.* **2006**, *44*, 1492–1501.
- (56) Srinivas, G.; Discher, D. E.; Klein, M. L. *Nature Mater.* **2004**, *3*, 638–644.
- (57) Won, Y.-Y.; Brannan, A. K.; Davis, H. T.; Bates, F. S. *J. Phys. Chem. B* **2002**, *106*, 3354–3364.